ORIGINAL ARTICLE

Geochemical appraisal of groundwater arsenic contamination and human health risk assessment in the Gangetic Basin in Murshidabad District of West Bengal, India

Debojyoti Mishra[1] · Kamaleah Sen[1] · Arghadip Mondal[1] · Soumya Kundu[1] · Naba Kumar Mondal[1]

Abstract

Geogenic arsenic is a metabolic hazard to global citizens, due to its presence in most of the rocks. Natural processes such as percolation of rainwater through soil layer and water–rock interaction in weathering process principally lead to the dissolution of arsenic-bearing minerals in the aquifer system. In the present study, arsenic (As)-contaminated groundwater was analyzed covering all blocks (26 blocks) of Murshidabad District, West Bengal, India. Principally, the study focused on the assessment of groundwater quality with respect to arsenic along with other metal ions such as iron, manganese, cadmium and selenium. Tube well water samples ($N = 348$) were collected during pre- and post-monsoon seasons. The spatial distribution of arsenic levels ranges from 0.086 to 0.513 mg/L in pre-monsoon and 0.059–0.431 mg/L in post-monsoon, which indicates that all groundwater samples of the Murshidabad District exceeds the WHO's permissible limit of arsenic (0.01 mg/L). Water quality index (WQI) data suggested that 5.74% and 10.3% samples are suitable for drinking purpose in the pre-monsoon and post-monsoon season, respectively. Availability of cations are as follows: $Ca^{2+} > Mg^{2+} > Na^+ > K^+$, and anions as: $SO_4^{2-} > HCO_3^- > Cl^- > F^- > NO_3^-$ in both pre-monsoon and post-monsoon seasons. Human health risk due to consumption of groundwater was assessed through USEPA designed methods as follows—hazard quotient (HQ), hazard index (HI), average daily dose of both direct ingestion of groundwater and dermal absorption of groundwater ($ADD_{Ingestion}$, $ADD_{Dermal\ absorption}$), and exposure frequency (EF). Thus, carcinogenic risk (CR) and non-carcinogenic risk (NCR) were determined. Results revealed that 29% and 37% of inhabitants suffered from carcinogenic and non-carcinogenic risk, respectively. On the basis of occurrence, spatial distribution and health risk assessment results of the targeted area can be marked as a moderate- to high-risk zone. The said zones need special attention for protection of public health.

Keywords Groundwater arsenic · Murshidabad District · Rock–water interaction · Inverse distance weighting · Water quality index · Health risk assessment

Introduction

Arsenic (As) is widespread in the world. It is the 20th most abundant element of the Earth's crust (Villalba et al. 2020). Arsenic pollution is a global threat; it is estimated that at least 230 million people in 107 countries access the arsenic-contaminated water above the World Health Organization (WHO) permission level of 0.01 mg/L (Chowdhury et al. 2000; Chowdhury et al. 2017; Shaji et al. 2021). The area of Asian countries, particularly the Ganga, Meghna, and Brahmaputra (GMB) river plains, are most affected by the threat of arsenic, which is the basin between India and Bangladesh (Chakraborti et al. 2017). At present, more than 100 million peoples in the GMB plain alone are at risk of potential groundwater arsenic contamination. Arsenic pollution (As > 0.01 mg/L) is found predominantly in groundwater, in aquifers of gray sand that were deposited onto a late Pleistocene landscape (McArthur et al. 2016). Pleistocene aquifers of central West Bengal at depth range > 70 m beneath paleo-interfluves contain 10–100 µg/L of arsenic (Bhowmick et al. 2012; Kulkarni et al. 2018; Majumdar et al. 2016). The sedimentary aquifers of the Bengal Delta Plain (BDP) belong to Bangladesh and neighboring West Bengal, where arsenic

✉ Naba Kumar Mondal
  nkmenvbu@gmail.com

1 Environmental Chemistry Laboratory, Department of Environmental Science, The University of Burdwan, Burdwan, West Bengal 713104, India

mobilizes through natural ways (redox processes, precipitation, absorption, and dissolution). Thus, the groundwater of the said areas become a major health issue related to environmental health concerns (Bhattacharya et al. 2004; Lim et al. 2014; Mazumder and Dasgupta 2011; Roy et al. 2014).

Arsenic interference may cause a number of abnormalities including restrictive pulmonary bronchiectasis, liver with non-cirrhotic portal fibrosis, polyneuropathy (Argos et al. 2010), anemia, peripheral vascular disease (PVD), hypertension, non-pitting edema of feet and hands, conjunctival congestion, etc. (Bera et al. 2010; Chowdhury et al. 2000; Mazumder and Dasgupta 2011). In addition, arsenic causes cancer in skin, but long-term exposure causes cancers of the bladder and lungs (National Research Council, US 1977; Shankar et al. 2014). The International Agency for Research on Cancer (IARC) has given guideline on arsenic and arsenic compounds as carcinogenic to humans and further states that arsenic in drinking water is carcinogenic to humans. Nevertheless, arsenic has uncovered the endemic arsenism that has had a detrimental effect not only on the health of millions of people, but also on their offspring in West Bengal (Bhowmick et al. 2018). Indeed, genotoxicity of inorganic arsenic results by reacting with sulphur containing compounds, generating both reactive oxygen species and nitrogen-containing species. Thus, epigenetically modified arsenic shows gene regulation along with methylation of DNA (Nava-Rivera et al. 2021). Accordingly, arsenic research is very essential based on geogenic sources, potential arsenic exposure, and health risk analysis in West Bengal. On the other hand, the increasing demand for groundwater leads to over-abstraction, a decline in groundwater levels and well yields, deteriorating water quality, and land subsidence (Nooria et al. 2021). As a matter of fact, the presence of 'As' in groundwater is not only related to the host minerals, but is also associated with sedimentation, which depends on the dissolved redox state and pH (Chakraborty et al. 2015). However, periodically deposits of arsenic are related to alluvial sedimentation and rich mineral ores belonging to the Holocene era (Bera et al. 2010; Chowdhury et al. 2000).

Previous research highlighted the association of arsenic with iron (Fe) and manganese (Mn) in Purbasthali, Burdwan (Ghosh et al. 2017). According to Ghosh et al. (2017), arsenic showed varying results with manganese, but iron showed a positive relationship. Recent studies (Ghosh et al. 2020 and Zhang et al. 2020) highlighted that both iron and manganese are highly responsible for increasing the hazard quotient (HQ) in arsenic-affected Padma River floodplains of Bangladesh due to their similar geochemical behavior, which reveals the natural presence of As and Mn in soil and aquifers. However, many factors such as depth, salinity, reducing environment, and contact time are responsible for dissolution of both iron and manganese in groundwater

(Carretero and Kruse 2015; Luzati et al. 2016). But most of the factors are untouched in previous literature.

The present study area, i.e. Murshidabad District, is situated more or less in the middle of West Bengal in which the Ganga River is majorly subdivided into two branches, i.e. Vagirathi (in India) and Padma (in Bangladesh) near Dhulian. So, Murshidabad District lies in the major floodplains of the River Ganga, where the majority of the areas are arsenic affected (3–3000 μg/L) (Halder 2019). The said district covers an area of 5324 km^2 and is densely populated with a total population of 5.9 million (as per census report 2011). Another point of concern about the Murshidabad District is the Holocene- and Pleistocene-aged dominating sediments, which are mainly constituted with Fe and Mn along with organic matter in aquifers of gray sand (Chatterjee et al. 2013; Neidhardt et al. 2014; Zhang et al. 2020). Therefore, it is expected that arsenic may easily mobilize in the reducing environment with the association of both iron and manganese (Kim et al. 2003; Rowland et al. 2005; Selim Reza et al. 2010; Wolf et al. 2009).

Earlier researchers such as Chowdhury and Paul. (2019), Dey et al. (2016), Haldar (2019), Majumdar (2018), Mondal et al. (1996), Rahman et al. (2005), and Samaddar et al. (2014) reported their study outcomes as quantification of groundwater as well as surface water arsenic level, health survey outcomes and population risk in selected areas of Murshidabad District. According to their research findings, there is still a lack of indepth study of the current scenario of arsenic vulnerability in Murshidabad District. Currently, the local people might be more exposed day by day, due to the geogenic arsenic toxicity. The present research work aimed to assess the arsenic and associated heavy metals (iron, manganese, cadmium, and selenium) -contaminated groundwater, which is consumed on a daily basis by the people of Murshidabad District, West Bengal. The study also assesses the distribution pattern of heavy metals through inverse distance weighting (IDW) mapping, water quality index, groundwater assessment, and human health hazard analysis and finally investigated the vulnerable zone of Murshidabad District leading to groundwater arsenic threat.

Materials and methods

Study area and sampling procedure

The study area of the present research is situated on the eastern peripheral plains to the middle of West Bengal, lying between 24º 50′ 20″ N to 23º 43′ 30″ N latitude and 88º 46′ 00″ E to 87º 49′ 17″ E longitude. The geological information of Murshidabad District was collected from Chatterjee et al. (2020) (Fig. 1B), which also describes two distinguished geological units such as fluvial sediment
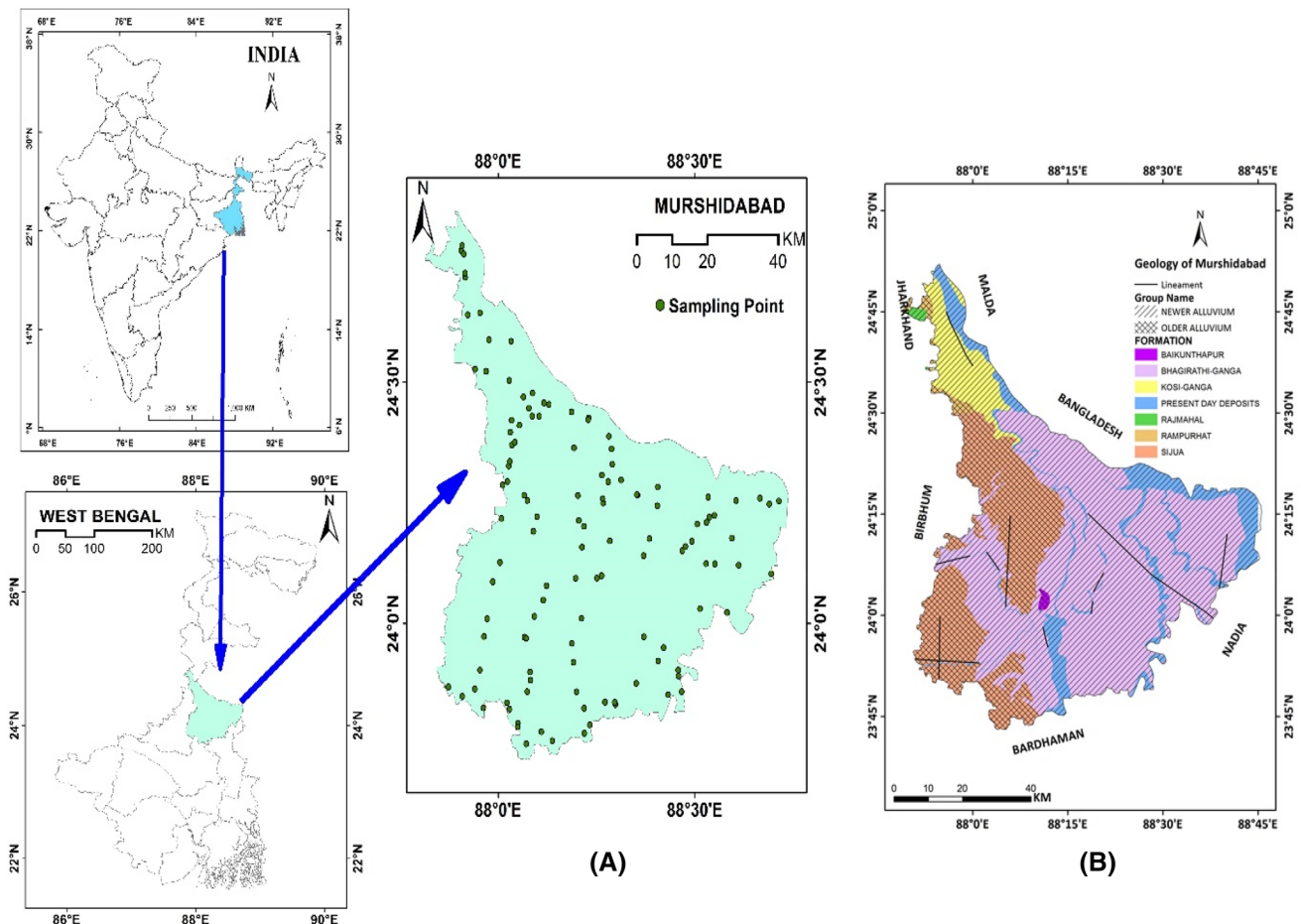
Fig. 1 **A** Study area map of Murshidabad District (sampling location), **B** Geological Map of Murshidabad District (Chatterjee et al. 2020)

and Rajmahal trap found in this region. Fluvial sediment belongs to Late Pleistocene- to Late Holocene-aged sand, silt and hard clay rock domains. The lithological unit of the said region shows semi-consolidated deltaic alluvium, ferruginous concretion, lithomarge clay gravels, pebbles, and cobbles. The aquifers of the said fluvial regions belong to high permeability, thick discontinuous aquifers. On the other hand, the Rajmahal trap lithological formation belongs to the Jurassic to Late Holocene-aged Rajmahal basalt, sand, silt, fine soft clays and hard clays impregnated with caliche nodules, whereas fairly thick regionally extensive confined/unconfined aquifers were located down to 3000 m. The said aquifers show unconsolidated fine sand and sandy silt with high to low permeability.

For the present study, groundwater samples were collected from both of pre-monsoon (March–May) and post-monsoon (September–November) season (Fig. 1 A). A total of 348 samples were collected (174 tube wells in each season) (Sahoo et al. 2018). The sampling process was carried out with one sample per 36 km^2 grid, covering (26 blocks of 5 subdivision) an area of 6264 km^2 located in Murshidabad

District, West Bengal (Chowdhury et al. 2000; Chakraborti et al. 2009). The depth of the tube well varied in the depth range of 24.38–106.68 m. The latitude and longitude of each sampling location were noted by using Oregon-750 handheld GPS, manufactured by- GARMIN. At the sampling spot, some background information was also noted, viz., type of rock around the sampling point, type of water that is consumable in higher quantity by the local people, is it drinkable or not, depth of water level (m) for groundwater, color and odor of the sample. The sampling bottles were dipped in soap water along with 3% HNO_3 overnight, and on the next day washed with distilled water (USEPA 2010). At the sampling spot, the bottles were again rinsed out with the respective water samples, and after that the water samples were collected. Separate samples were collected and preserved with a few drops of concentrated HNO_3 for heavy metal analysis.

Physicochemical parameter analysis

Physicochemical parameters such as temperature, pH, dissolved oxygen (DO), total dissolved solids (TDS), salinity, conductivity, oxidation reduction potential (ORP) and anions such as chloride, fluoride, and nitrate were measured by Multiparameter (Thermo Fisher Scientific—ORION STAR A329). Different electrodes were used for different parameters. Initially, the instrument was calibrated by standard protocol. Measurements of the total hardness, total alkalinity, phenolphthalein alkalinity, carbonate and bicarbonate were measured by the titrimetric method, by following standard methodologies (Chakraborti et al. 2009; Prathap and Chakraborty 2019). On the other hand, sulphate and phosphate were measured by the spectrophotometric method (Systronics-104) (APHA 2005).

Heavy metals and cation analysis

Arsenic, iron, manganese, cadmium and selenium were measured by atomic absorption spectrophotometer manufactured by, Lab India (AA 8000). The water samples were digested through the triacid digestion method, followed by filtration through Whatman 42 filter paper. The respective standards of stock solution and the filtrate samples were prepared for analysis. Cations like calcium, magnesium, sodium, potassium, lithium and ammonium were measured by Ion-chromatography (IC) (Thermo Fisher Scientific-17050089). Each water sample filtrated through Agilent manufactured filter cap, and injected into the IC machine.

Inverse distance weighting (IDW) mapping

Water samples' experimental data were compared with the interpolation technique, namely inverse distance weighting (IDW) to generate the spatial distribution mapping of ORP, As, Fe, Mn, Cd, and Se in groundwater for both the pre- and post-monsoon season. The mapping was conducted through 'Arc GIS' software (Version-10.3). The IDW is a deterministic interpolation method in the field of groundwater hydrology, made from located sampling areas. It gives more weights to data points closest to the prediction location, and the weights shrink as a function of distance. Subsequently, measured values those are adjoining to the prediction location have greater influence on the predicted value than of distant points (Adhikary and Dash 2014). The choice of this weighting power can significantly affect the estimation quality. The optimal weighting power depends on the spatial structure of the data and is influenced by the coefficient of variation (CV), skewness and kurtosis of the data (Gotway et al. 1996; Mueller et al. 2001). Therefore, the sampling data are interpolated by the following mathematical equation to generate IDW mapping.

$$Z(x_0) = \frac{\sum_{i=1}^{n} \frac{x_i}{h_{ij}^{\beta}}}{\sum_{i=1}^{n} \frac{1}{h_{ij}^{\beta}}}, \tag{1}$$

where $Z(x_0)$ represents the interpolated data, 'n',x_i, h_{ij}, and β are denoted as sample size values, the ith data value, the separation distance between the interpolated value and the sample data, and the weighting power, respectively.

Groundwater modeling

Following the objectives of the present study, two types of groundwater modelling (Piper trilinear diagram and Gibbs' diagram) are applied to observe the hydrogeochemistry of the groundwater of Murshidabad District. The dominancy of cations and anions in groundwater for the both pre- and post-monsoon season were accomplished through a Piper trilinear diagram (Piper 1944). The diagrams were carried out through XLSTAT software (2020.1). Whereas, Gibbs' diagram was applied to observe the geochemical water–rock interaction that occurred due to precipitation and evaporation. These diagrams were also plotted through XLSTAT software, to understand the overall quality and the maturity of the groundwater. Water quality index (WQI) was calculated based on 18 physicochemical parameters. The parameters such as cations (As, Fe^{2+}, Mn^{2+}, Na^+, Ca^{2+}, K^+, Mg^{2+}, Cd^{2+}, Li^{2+}, Se^{2+}, NH^{4+}), anions (Cl^-, F^-, NO_3^-, SO_4^{2-}, HCO_3^-, PO_4^{3-}), pH, DO, ORP, EC, total alkalinity, salinity, TDS and total hardness were estimated for this study. The water quality index was calculated by using the following Eq. (2):

$$W_i = QW_i / \sum_{i=1}^{n} W_i, \tag{2}$$

where Q was computed using the determined concentration of the groundwater parameter,

[$Q = (C_i/S_i) \times 100$], C_i = specific parameter's concentration in mg/L, S_i = the permissible value prescribed by Bureau of Indian Standards (BIS) in mg/L, and W_i are computed values for the groundwater parameter.

Human health risk analysis

Good quality of drinking water is important for human health and quality of life. The natural and anthropogenic activities are responsible for arsenic contamination in groundwater and their incidence is recognized as a major public health issue. The evaluation of human health risk assessment of such heavy metal is becoming mandatory to understand the potential harmful impacts beyond the assessment of heavy metal concentrations (Adimalla and

Qian 2019; Ekoa Bessa et al. 2020). Quantitative assessment of both carcinogenic and non-carcinogenic risk assessments was performed by following the standard methodology (USEPA 1989). Similarly, non-carcinogenic risk of the hazard quotient (HQ) considering ingestion and dermal contact to arsenic contaminant groundwater was also assessed. The hazard index (HI) was computed by the sum of dermal absorption and ingestion of groundwater. Reference dose (RfD) and cancer slope factor (CSF) are helpful in the estimation of the carcinogenic risk (CR) (Duggal and Rani 2018; USEPA 1989). Herein, HQ was calculated by applying the following equation (Eq. 3):

$$HQ = \frac{ADD}{RfD}, \tag{3}$$

where ADD and RfD are average daily dose ADD (mg/kg day^{-1}) between ingestion of groundwater and dermal absorption of groundwater (ADD$_{dermal}$ and ADD$_{ingestion}$) and reference dose (RfD), respectively. RfD is the ingestion of groundwater (30 mg/kg day^{-1}) or dermal contact to groundwater (28.5 mg/kg. day^{-1}) exposure (Hossain and Patra 2020; USEPA 2004).

$$ADD_{dermal} = \frac{K_p \times C_{DGT} \times ET \times ED \times SA \times 10^{-3}}{BW \times AT \times EF}. \tag{4}$$

From Eq. 4, K_p, C_{DGT}, ET, EF, ED, SA, BW and AT are the dermal permeability coefficient (0.001 cm/h), As concentration in water (mg/L), time of exposure (0.5 h/day), exposure frequency (365 day/year), exposure duration (30 years), exposed skin surface (18,000 cm^2), average body weight (70 kg), and mean time (30 years), respectively (USEPA 2010).

$$ADD_{ingestion} = \frac{K_p \times CSF \times C_{DGT} \times ET \times AT \times SA}{BW \times ED \times EF}. \tag{5}$$

In Eq. 5, the relative parameters are K_p (permeability coefficient at 0.001 cm/h), ET (exposure at 0.5 h/day), CSF (cancer slope factor), C_{DGT} (arsenic concentration in water unit mg/L), IR (ingestion rate at 2 L day^{-1}), EF (exposure frequency in 365 days year^{-1}), ED (exposure duration in 30 years), SA (exposed skin surface on 18,000 cm^2), BW (body weight at 70 kg), and AT (average time 30 years). The HI was calculated as the sum of HQ dermal contact to groundwater and HQ ingestion of groundwater (USEPA 2004, 2010, 2012), Carcinogenic risk (CR) assessments (USEPA 2010, 2012) are expressed according to the following equation:

$$CR = ADD \times CSF. \tag{6}$$

Herein, the carcinogenic risk was obtained through the average daily dose (ADD) with cancer slope factor (CSF). The CSF was obtained from the chemical potency and specialized various contaminants (Mondal 2020). The carcinogenic risk enhancement tendency increases linearly with the chemical dose. CSF is subjected to actual research that reflects health problems from certain levels of carcinogenic contaminants. The CR has accessible ranges between 10^{-6} and 10^{-4} of US EPA, measuring through sampling on a particular basis.

Statistical analysis

The experimental data were statistically evaluated by using MINITAB 16 software to determine various statistical interrelation along with their significance. All physicochemical parameters and cation and anion concentrations were reported as the mean, standard deviation, minimum and maximum. Pearson correlation was performed with arsenic and subsequent heavy metals: iron, manganese, selenium and cadmium (Fig. 5S). The probability values of $p < 0.01$ and $p < 0.05$ were considered to be significant for comparison of different data sets of two seasonal data. Through multiple linear regression analysis, the effects of independent variables such as cations, anions and depth of groundwater sample were observed with the dependent variable, i.e. arsenic. The variability of human health risk due to groundwater arsenic was carried out through probabilistic model by Monte Carlo simulation (Hossain and Patra 2020; Sohrabi et al. 2020). The said simulation diagram was performed by using Oracle Crystal ball software (11.1.2.4) to estimate the validity of carcinogenic risk depending on the 5% and 95% percentile quartile probabilistic approach.

Results and discussion

Physicochemical characteristics of the groundwater

The physicochemical characteristics of the groundwater of Murshidabad District are depicted in Table 1. Water quality data clearly demonstrated that the pH of the groundwater lies between neutral to faintly alkaline range in both premonsoon (6.41–8.74) and post-monsoon (6.5–8.5) seasons. The pH of the groundwater varies due to the composition of minerals in the surrounding rocks near the water table and constituents of lithological unit in the groundwater recharge zones (Nakagawa et al. 2021), whereas the alkaline nature of groundwater samples is supposed to be due to the availability of cationic species (Chowdhury and Paul 2019; Kumar et al. 2010; Rahman et al. 2005). Total 0.017% and 0.005% of the studied samples exceeded the WHO permissible limit of pH (8.5) in both the pre- and post-monsoon seasons, respectively. In the studied areas of 26 blocks of Murshidabd District, the higher level of pH (> 8.5) was recorded in the blocks of Burwan (Kaitha), Nabagram

Table 1 Statistical summary of groundwater parameters (major and trace elements; $n = 348$, i.e. 174 in both pre- and post-monsoon)

Parameters (units)	Pre-monsoon			WHO limit	Post-monsoon		
	Minimum	Maximum	Mean ± SD		Minimum	Maximum	Mean ± SD
pH	6.41	8.74	7.537 ± 0.354	6.5–8.5	6.400	8.500	7.762 ± 0.296
TDS (mg/L)	115.77	827.10	353.011 ± 128.39	1000	22.80	792.6	264.453 ± 134.90
Conductivity (µS/cm)	291.7	1667.0	719.611 ± 257.8	2.0	300.7	1616.3	540.207 ± 270.50
Temperature (°C)	26.60	32.200	25.370 ± 0.995	–	22.20	28.20	33.629 ± 2.600
ORP (mV)	227.20	578.30	292.557 ± 104.06	–	356.00	658.20	418.196 ± 56.070
Salinity (mg/L)	177	794	438 ± 0.115	–	194	569	287 ± 0.432
DO (mg/L)	4.02	6.090	5.844 ± 0.421	14	0.188	7.654	5.049 ± 0.865
Total Hardness (mg/L)	9.20	92.05	31.779 ± 6.72	500	8.400	100.80	16.149 ± 14.850
Total Alkalinity (mg/L)	20.01	88.23	46.712 ± 13.72	–	16.03	88.11	50.505 ± 15.38
F^- (mg/L)	0.033	2.101	0.427 ± 1.585	1.5	0.109	5.750	0.039 ± 0.466
HCO_3^- (mg/L)	20.00	88.00	46.712 ± 13.72	500	16.11	88.29	50.505 ± 15.38
Cl^- (mg/L)	0.070	440.22	36.719 ± 65.07	250	0.070	983.01	22.558 ± 85.12
SO_4^{2-} (mg/L)	1.110	175.56	54.312 ± 37.57	500	0.371	226.30	48.607 ± 44.90
PO_4^{3-} (mg/L)	0.589	6.532	4.838 ± 1.081	---	0.236	10.589	2.332 ± 2.526
NO_3^- (mg/L)	0.008	1.300	6.658 ± 0.331	---	1.130	33.400	0.398 ± 6.761
Na^+ (mg/L)	0.198	19.138	2.798 ± 2.946	200	0.280	20.912	5.134 ± 2.235
K^+ (mg/L)	2.334	44.159	1.309 ± 3.659	200	0.0412	6.300	1.543 ± 1.128
Mg^{2+} (mg/L)	0.005	11.667	1.523 ± 2.309	150	0.008	9.300	1.604 ± 1.512
Ca^{2+} (mg/L)	0.114	26.289	1.819 ± 4.214	100	0.001	14.200	3.369 ± 2.591
NH_4^+ (mg/L)	0.002	0.990	0.144 ± 0.144	---	0.00012	1.080	0.058 ± 0.223
Li^+ (mg/L)	0.002	0.820	0.048 ± 0.083	---	0.00022	0.600	0.034 ± 0.103
Total Arsenic$^+$ (mg/L)	0.086	0.514	0.190 ± 0.065	0.01	0.0550	0.432	0.207 ± 0.073
Cd^{2+} (mg/L)	0.001	0.205	0.006 ± 0.021	0.005	0.0001	0.117	0.009 ± 0.017
Total iron (mg/L)	2.007	98.144	12.094 ± 7.374	0.3	1.8760	80.019	12.595 ± 9.981
Mn^{2+} (mg/L)	0.029	0.437	0.112 ± 0.069	–	0.0150	0.360	0.153 ± 0.056
Se^{2+} (mg/L)	0.0001	0.014	0.005 ± 0.0034	0.01	0.0001	0.137	0.004 ± 0.016

(Ikrol, Ayra, Bilbari), Sagardighi (Bhurkunda, Gokulta), Beldanga-II (Ramnagarghat, Jainagar, Nazipur, Kulbaria), Kandi (Hijal), Berhampore (Simulia, Mahala, Chumaigacha, Komnagar), Nawda (Sarbangapur, Gohat), Khargram (Khargram, Kapasdanga), and Bharatpur-II (Angarpur, Gidgram, Rautari, Alepur, Salar, Kagram). Earlier studies (Bhowmick et al. 2012; Chatterjee et al. 2013; Chakraborti et al. 2009) reported the existence of both As (III) and As (V) in groundwater within the pH range between 6 and 9 and are mainly accommodated in anoxic and oxic water, respectively. Very recently, Shaji et al. (2021) demonstrated a strong positive relationship between water alkalinity and As level in groundwater. However, both arsenic species can also co-exist in oxic and anoxic aquifer as H_2AsO_2—and $HAsO_2^{2-}$ in pH 5–7 range (Andersen et al. 1991; Kim et al. 2003). On the other hand, the mobility and persistence of various geogenic contaminants depend on the redox nature of groundwater (Knierim et al. 2021). Hence, oxidation reduction potential (ORP) is also a valuable determining factor for proper understanding of arsenic availability in groundwater. Results also revealed that in the pre-monsoon season, water samples are oxic in nature compared to the post-monsoon session, and the level of arsenic load is 33% higher in the pre-monsoon than the post-monsoon. However, previous reports did not highlight such strong coherency between ORP and groundwater arsenic level (Kulkarni et al. 2018; Majumdar et al. 2016; Mandal et al. 1996; Planer-Friedrich et al. 2012).

Again, hardness in groundwater occurs due to divalent cations. Nevertheless, the availability of cations in groundwater is not only a deterministic factor to identify the characteristics of softness or hardness, but also a key element leading to TDS and EC (Mahato et al. 2018). The present study results revealed that the mean hardness level, electrical conductivity and TDS values showed almost threefold increase in post-monsoon compared to pre-monsoon. This may be due to the effect of precipitation in monsoon which may lead to the increase of electrical conductivity and TDS (Chatterjee et al. 2013; Ghosh and Rolee 2011; Rahman et al. 2005; Samaddar et al. 2014). Moreover, the abundance of ionic species in the post-monsoon season is due to the enrichment on chemical weathering and lengthier residence time (Chatterjee et al. 2013; Ghosh and Rolee 2011). The availability

of bicarbonate (HCO_3 –) ions in two seasons is more or less the same due to dissolution of CO_2 and carbonates (Chakraborti et al. 2009; Kumar et al. 2010). Again, pyrite oxidation leads to the dominancy of carbonate/bicarbonate and this oxidation of pyrite also dissolves Fe-oxyhydroxide and releases the ions of bicarbonate which trigger the contamination pattern of As during the recharging time (Alam et al. 2016; Bindal and Singh 2019, Choudhury and Paul 2019; Ghosh et al. 2020; Kumar et al. 2010; Planer-Friedrich et al. 2012). The main mechanism of arsenic in groundwater may be the dissolution of arsenic sulphide minerals (arseno-pyrite) (O'Day et al. 2004). On the other hand, enrichment of sulphur is due to the oxidation of pyrite and reduction of SO_4^- through the diagenesis mechanism during sediment deposition (Herath et al. 2016; Wu et al. 2020). The present results show almost double concentration of sulphate in the post-monsoon season compared to the pre-monsoon season. Similarly, mean nitrate concentration in the post-monsoon samples is remarkably higher than the pre-monsoon season. The nitrate enrichment in groundwater may be due to the reduction of sedimentary organic matter by denitrifying microorganisms and the base-flow mechanism in the river basin near aquifer (Anning et al. 2012; Beisner et al. 2012; Dey et al. 2016; Knierim et al. 2021; Planer-Friedrich et al. 2012). The mean F^- and Cl^- level is about three times higher in post-monsoon compared to pre-monsoon season. However, most of the samples lie within the permissible limit of WHO. In post-monsoon, fluoride and chloride availability may be the result of precipitation (Chatterjee et al. 2013).

Previous studies (Chowdhury and Pal 2019; Kulkarni et al. 2018; Planer-Friedrich et al. 2012) clearly demonstrated that the distribution of arsenic in groundwater greatly varies with depth. In the present study, water samples were collected from different depths (25–106 m) and it was estimated that about 36%, 59% and 5% samples were collected from < 30 m, < 60 m and < 106 m depth, respectively. The level of arsenic varies between 0.108–0.304 mg/L and 0.055– 0.302 mg/L during pre-monsoon and post-monsoon in lower depth shallow aquifer (< 30 m); 0.086–0.514 mg/L and 0.069–0.432 mg/L during pre-monsoon and post-monsoon in moderate depth aquifer (< 60 m); 0.099–0.239 mg/L and 0.098–0.206 mg/L during pre-monsoon and post-monsoon in higher depth deep aquifer (< 106 m), respectively. These results clearly indicate that shallow aquifers are more vulnerable than deeper aquifer (Kulkarni et al. 2018; Majumdar et al. 2016; Mandal et al. 1996). The existence of a clay layer within the aquifer may be responsible for the existence of As in groundwater (Liu and Wu 2019). Moreover, the existence of black shale or pyrite in the soil strata is the main source of As. According to Maliva (2019), excessive withdrawal of groundwater leads to oxidizing environment in groundwater, which supports the release of arsenic from arsenic-rich iron oxyhydroxide. The present results

also suggested that the mean value of iron is almost double in the post-monsoon season, whereas the mean manganese level depicts almost fourfold decrease in the post-monsoon season compared to the pre-monsoon season. This may be attributed to the effects of dispersion by the colloidal aggregates, which are subsequently responsible for dilution of recharge water (Cheng et al. 2005; Ghosh et al. 2020; Planer-fridrich et al. 2012; Zhang et al. 2020). Similarly, in Bharatpur-II (Salar) area, the levels of As, Fe and Mn were recorded as 0.514 mg/L, 47.589 mg/L and 0.34 mg/L, respectively. These data suggest that arsenic showed good consistency with both iron and manganese. As far as the geological setting of Murshidabad Districts is concerned, the dominating sediments are of the Holocene and Pleistocene Age and mainly constitute Fe and Mn along with organic matter (Chatterjee et al. 2013; Neidhardt et al. 2014; Zhang et al. 2020). It is also observed that the nature of Bengal basin aquifer water turns to reddish yellow after a short duration of aerial contact which indicates a reducing environment. Therefore, it is expected that arsenic may easily mobilize under such reducing environment (Kim et al. 2002, 2003; Rowland et al. 2005; Selim Reza et al. 2010; Wolf et al. 2009).

The presence of cationic load also varied in the post-monsoon season in comparison to the pre-monsoon period. The results demonstrated that the mean concentration of Na^+ and K^+ decreased by sevenfold, whereas two times decrease of Mg^{2+} ions were observed during post-monsoon, along with 66% and 14% decrease of Ca^{2+} and NH_4^+ ions, respectively. The decreasing pattern may be due to mixed up consequences, i.e. low-oxygen condition when anaerobic bacteria are present and low permeability in the aquifer material of the soil. (Mohammed-Aslam and Rizvi 2020; Singh. et al. 2015). On the other hand, two times increase of Cd^{2+} and 14% increase of Se^{2+} were recorded, whereas 25% increase of Li^{2+} concentration was found in the post-monsoon period. The increasing phenomena may bes due to surface water runoff, causing groundwater contamination with a variety of pollutants generated from agricultural land (Kumaresan and Riyazuddin 2006). Previous researchers (Borah et al. 2018; Ghosh and rolee 2011; Gogoi et al. 2016) also demonstrated a similar variation of anionic species and argued that precipitation and sedimentary complexion were the main sources behind the lower concentration of cations or anions.

Ionic constituents of the groundwater and their probable controlling mechanism

Hydrogeochemical facies of ions distribution and genesis are demonstrated in Fig. 2. The hydrogeochemical regime highlighted the abundance of several ionic species including cations (Ca^{2+}, Mg^{2+}, Na^+ and K^+) and anions (HCO_3^-, SO_4^{2-} and Cl^-). The ionic abundance of the seasonal
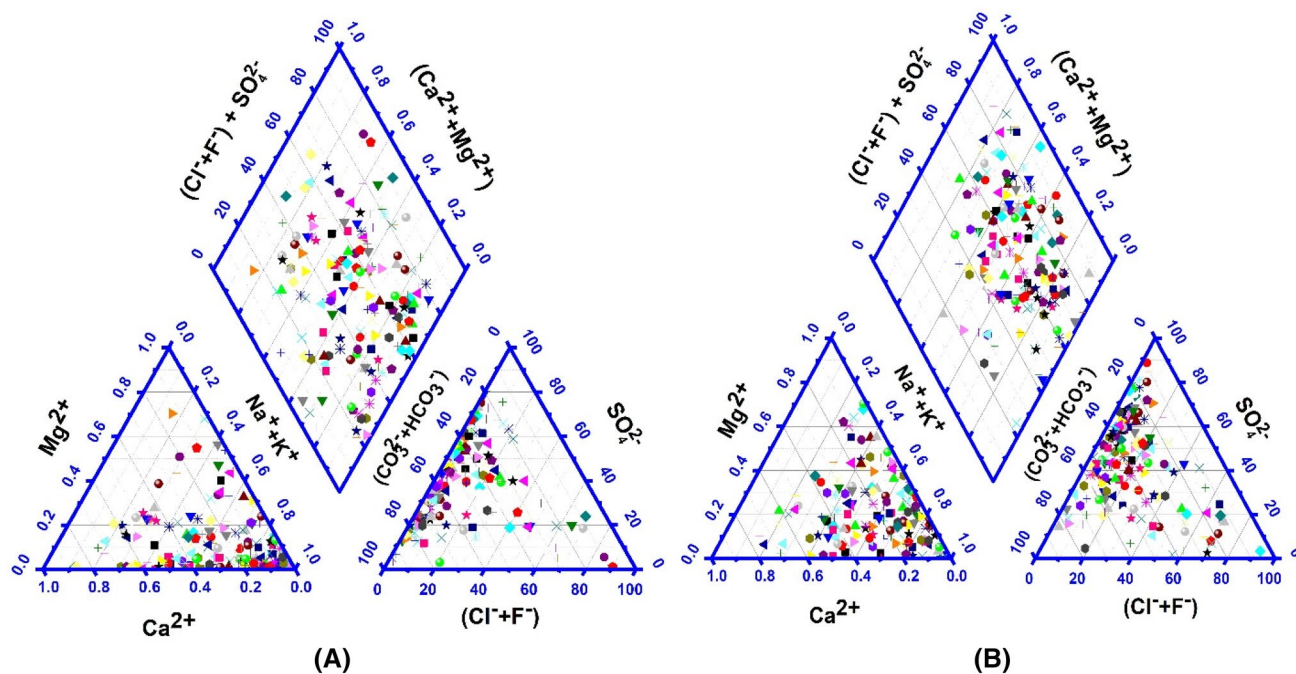
Fig. 2 Piper diagram for representing chemical analysis of groundwater in **A** pre-monsoon, **B** post-monsoon

variation is principally dominated by hydrochemistry of rock–water interaction (Kulkarni et al. 2018; Alam et al. 2016). During rock–water interaction, a mixture of chemical phenomena occur, i.e. weathering and dissolution, ion exchange processes, oxidation and reduction (Herath et al. 2016). As a result, it can observed that ionic constituents may increase or decrease, depending upon mobility and pH of the medium (Dehnavi et al. 2011). Moreover, Piper diagram clearly demonstrates the mixture of water chemistry which is important towards understanding the possible sources of dissolved constituents in water. In pre-monsoon, the species availability is Ca–HCO_3, Na–Cl, Ca–Mg–Cl, Ca–Na–HCO_3 and Ca–Cl. The upshot of the cation and anion interaction is mainly dominated during the pre-monsoon season as Ca–Mg–HCO_3 type in the Piper diagram, which is supposed to be derived from the weathering and dissolution of major rocks such as quartzite, hornblende biotite gneiss, charnockite and pyroxenes (Alam et al. 2016; Kumar et al. 2010). Seasonal variation of cations is mainly dominated due to geogenic activity (Wu et al. 2020). Various forms of arsenic in groundwater is due to young Asian deltaic aquifers, along with interaction of unsaturated sandy sediments during rainy season through percolation (Chatterjee et al. 2013; Chakraborty et al. 2009; Kulkarni et al. 2018; McArthur et al. 2016). Similarly, in the post-monsoon season, the major interaction type is Na–Cl. This is due to loading of rainwater from localized collection and by ion's mitigation from rocks. However, Alam et al. (2016) explained that the exchange process of Ca^{2+}

and Na^+ ions is dominated by the geochemical process for Na–Cl type. The present research highlighted that the dominating cations are $Ca^{2+} > Mg^{2+} > Na^+ > K^+$ and anions are $SO_4^{2-} > HCO_3^- > Cl^- > F^- > NO_3^-$. The Gibbs diagram (Fig. 3) explains the aquifer lithology and water chemistry, plotted by TDS against $Cl^-/(Cl^- + HCO_3^-)$ and $(Na^+ + K^+)/(Na^+ + K^+ + Ca^{2+})$. Figure 3 also helps to understand three distinct dominance areas such as precipitation, evaporation and rock–water interaction (Gibbs 1970). From Fig. 3 (A and B: anions and C and D: cations), it has been observed that the majority of the samples fall in the field of rock–water interaction dominance during both pre- and post-monsoon seasons. Therefore, these results signify the interaction between rock and percolated water under the subsurface (Kumar et al. 2015; Prathap and Chakraborty 2019). The results indicate that both pre- and post-monsoon seasons can cause rock erosion and dissolution of mineral phenomena during percolation from the subsurface, mineral dissolution of carbonate and silicate along with granitic gneiss minerals.

Analysis of spatial distribution of arsenic with relative parameters using inverse distance weighting (IDW) maps

Inverse distance weighting (IDW) is the deterministic method corresponding to multivariate interpolation by marginal scatter set (Yang et al. 2020). The IDW diagrams of oxidation reduction potential (ORP) of the study area of Murshidabad District are depicted in Fig. 1S. From Fig. 1S,
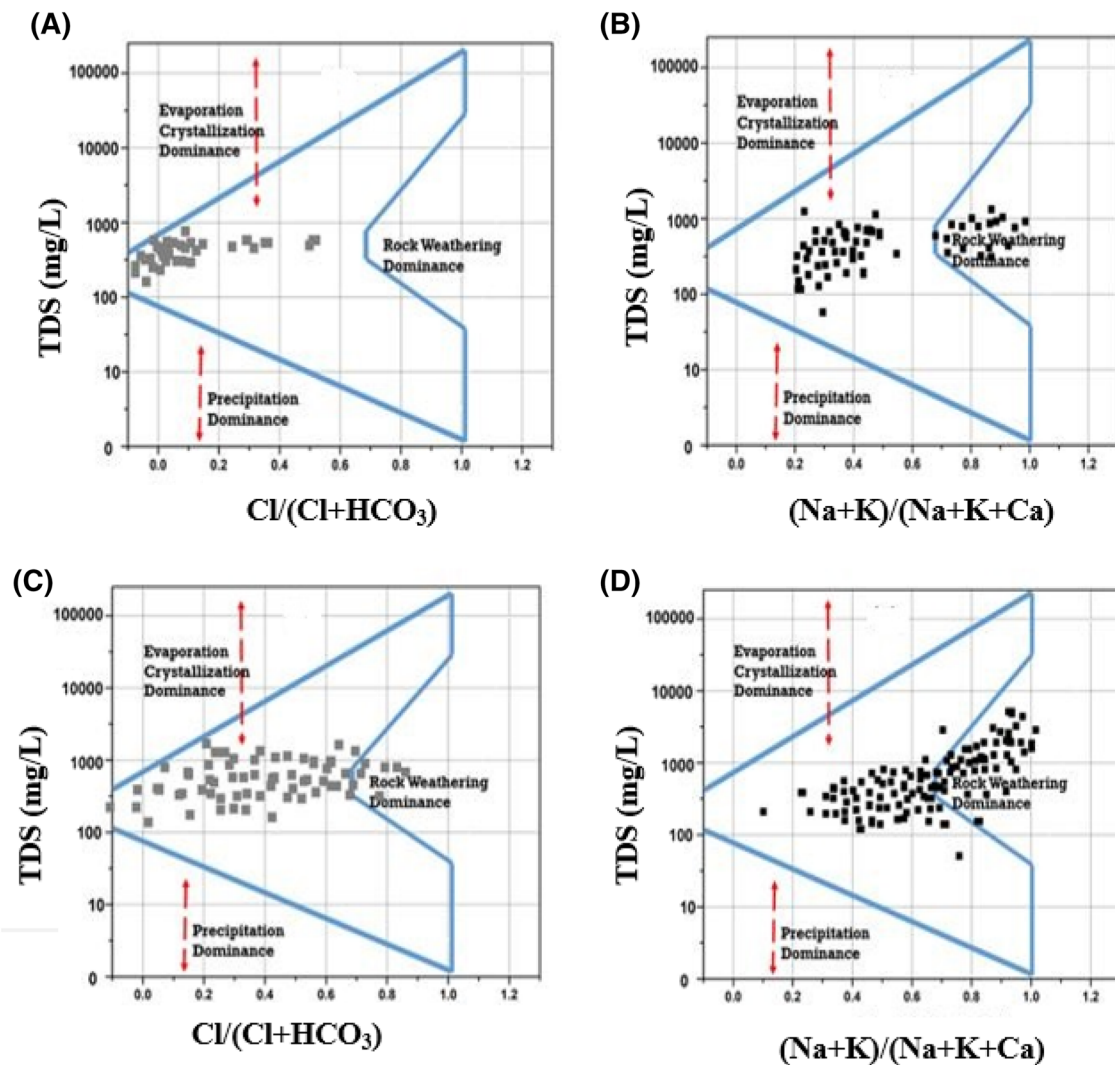
Fig. 3 Gibbs diagram showing the rock–water interaction of the groundwater in pre-monsoon and post-monsoon (**A** and **B**: an ions and **C** and **D**: cations)

it has been observed that the mean ORP (mV) is two times higher in post-monsoon (418.196 ± 56.07) compared to pre-monsoon (292.557 ± 104.06). The higher ORP in the post-monsoon season is probably due to the higher precipitation rate and the mineral saturation index (Elumalai et al. 2017). ORP is high owing to cationic substances (As, Fe, Mn) involved in oxidation, which supports the mineral dissolution of cation (Shrivastava et al. 2014). In the pre-monsoon season, minerals become precipitated due to low solubility. However, in post-monsoon, higher levels of minerals signify higher solubility, which results in higher ORP value. Rainfall significantly affects the As concentration in the different parts of the world (Shaji et al. 2021). The present study revealed that arsenic level is higher in pre-monsoon than post-monsoon. This is probably due to low ORP in pre-monsoon indicating reducing environment, which is responsible

for dissolution of arsenic-bearing minerals (Singh and Singh 2018). Again, it can be seen from Fig. 4 that the distribution of arsenic is random in nature**.** This is possible due to the drainage pattern of Ganges River or alluvial deposition, which may lead to a major switch to contamination when recharging during the post-monsoon season. Therefore, these random spots of high As occurrence need urgent attention to be monitored. Fundamentally, these zones are vital to identify those areas which are responsible for contamination of arsenic in groundwater.

The level of arsenic in groundwater in the study area was recorded as 0.086–0.514 mg/L in pre-monsoon and 0.059–0.432 mg/L in post-monsoon. Therefore, these data clearly mention that 100% of water samples exceed the WHO's recommended levels in both pre- and post-monsoon. The iron contamination zone in the post-monsoon
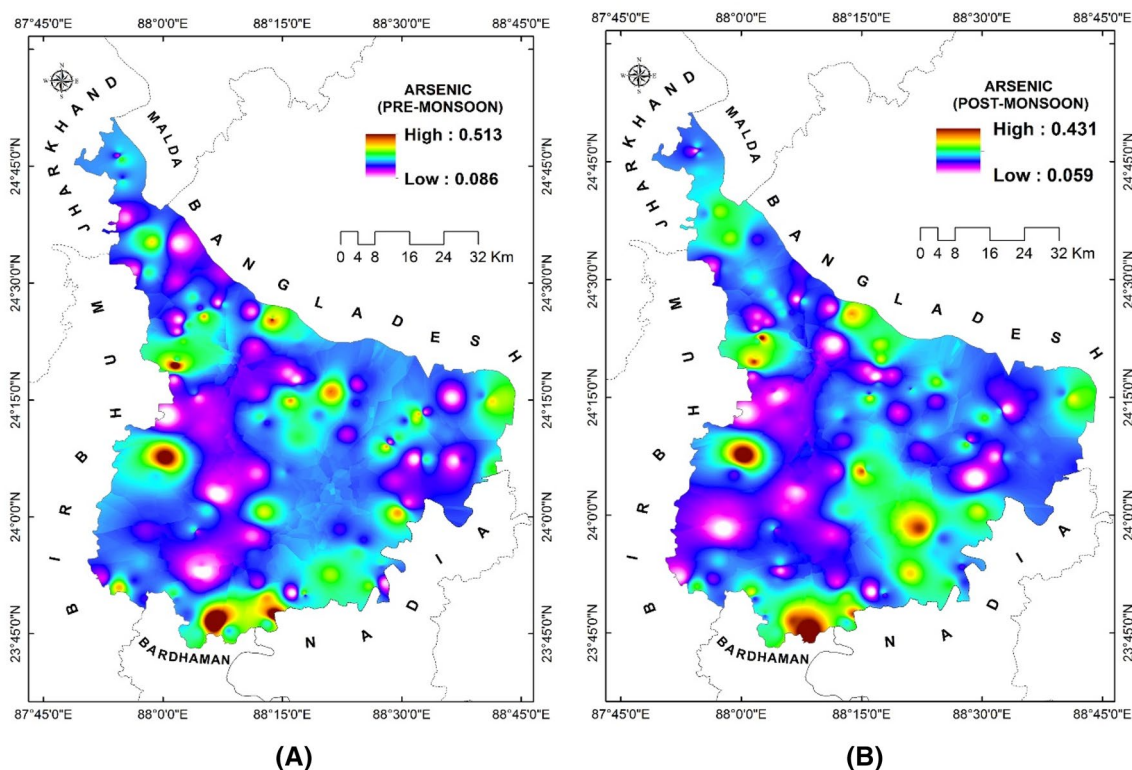
Fig. 4 Spatial distribution of arsenic concentration in groundwater (mg/L) (**A**: pre-monsoon, **B**: post-monsoon) in Murshidabad district

season is slightly higher and similar to arsenic and manganese zone (Fig. 5). The arsenic recognized zone of Bharatpur-II, Burwan, Khargram, Beldanga-II, Raninagar-II, Berhampore, Domkol and other areas also showed higher level of iron and manganese in groundwater. However, both selenium and cadmium levels showed higher concentration in post-monsoon than pre-monsoon (Fig. 2S and 3S). According to water quality index (WQI) value, water can be categorized as excellent (0–25), good (26–50), poor (51–75), very poor (75–100), and WQI value above 100 is unsuitable for drinking water (Khan and Kumar 2013). The present WQI results revealed that in pre-monsoon season, 5.74%, 46%, 33%, 14% water samples were excellent, good, poor and very poor, respectively, and 1.26% samples were not suitable for dinking. Similarly in post-monsoon season, 10.3%, 50.7%, 28%, and 10% water samples were excellent, good, poor and very poor, respectively, and 1% samples not suitable for dinking, respectively. Figure 4S demonstrates the spatial distribution of arsenic in Murshidabad District by IDW interpolation in the pre-monsoon and post-monsoon seasons. The yellow patches of these figure clearly indicate the worse quality of water and it is unsuitable for drinking. Therefore, particularly these yellow marked areas need special care for management.

Pearson correlation study

Pearson correlation among the various physicochemical parameters of ground water were done for both pre-monsoon and post-monsoon seasons and is presented in Tables 2 and 3. From Table 2, it is observed that groundwater arsenic level significantly correlated with bicarbonate ($r = 0.951$, $p < 0.001$), iron ($r = 0.739$, $p < 0.001$) and EC ($r = 0.884$, $p < 0.001$) and significant negative correlation was recorded with chloride ($r = -0.637$, $p < 0.001$), nitrate ($r = -0.729$, $p < 0.002$) and fluoride ($r = -0.346$, $p < 0.004$) in pre-monsoon season. Similarly, during post-monsoon season, arsenic showed significant positive relationship with bicarbonate ($r = 0.443$, $p < 0.031$), sulphate ($r = 0.886$, $p < 0.005$), iron ($r = 0.883$, $p < 0.001$) and EC ($r = 0.822$, $p < 0.066$). In addition, arsenic showed a strong negative relation with nitrate ($r = -0.821$, $p < 0.001$) and chloride ($r = -0.855$, $p < 0.066$) (Table 3). Strong correlation of arsenic with bicarbonate may indicate the presence of $CaCO_3$ mineral. The bicarbonate ions can neutralize the H^+ or OH^- ions, by substituting arsenic bearing minerals arsenite (As 3^+), which lead the mobility of arsenic in groundwater (DeVore et al. 2019). The higher level of nitrate and sulphate in post-monsoon probably happens due to the presence of denitrifying organisms and rock–water interaction by pyrite (FeS_2) subsequently
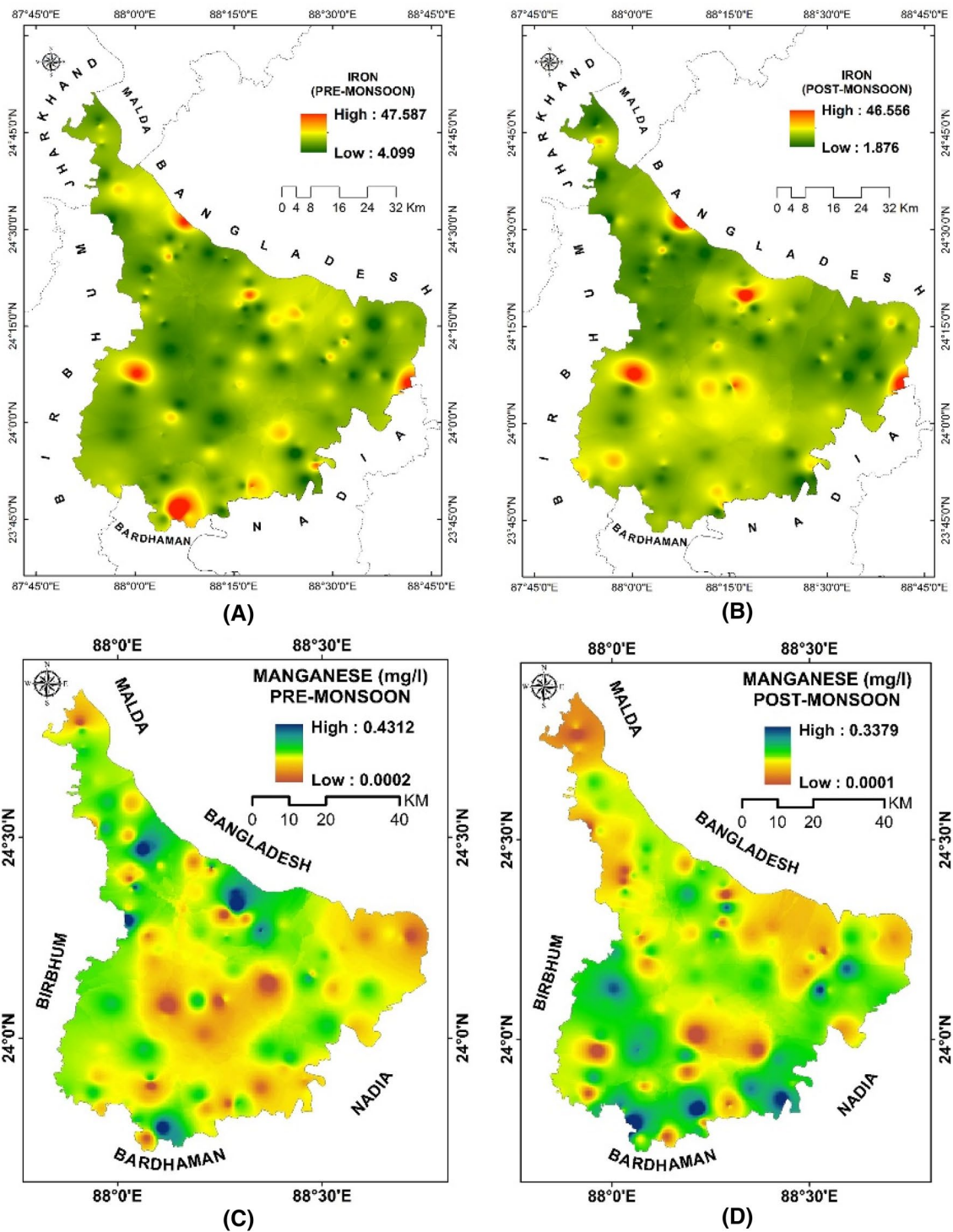
Fig. 5 Spatial distribution of iron concentration in groundwater (mg/L) (**A**: pre-monsoon, **B**: post-monsoon) and manganese concentration in groundwater (mg/L) (**C**: pre-monsoon, **D**: post-monsoon) in Murshidabad district

(Natasha et al. 2020). Hence, bicarbonate-containing minerals are possibly responsible for the availability of arsenic in the groundwater (Rasool et al. 2016). Similarly, correlation results also revealed that irrespective of season, arsenic showed statistically significant relation with total iron (Roy et al. 2013). Similar results were reported by Ghosh et al. (2020) in their recent study in the arsenic-contaminated areas of Bangladesh.

Table 2 Pearson correlation among the various physicochemical parameters of groundwater in the pre-monsoon season ($n = 174$)

	As (mg/L)	Bicarbonate (mg/L)	Cl⁻ (mg/L)	EC (µS/cm)	F⁻ (mg/L)	Fe (mg/L)	NO₃⁻ (mg/L)	ORP (mV)	pH	PO₄³⁻ (mg/L)	Salinity (ppm)	SO₄²⁻ (mg/L)	TDS (mg/L)	Temp. (°C)	Total alkalinity (mg/L)	Total hardness (mg/L)
Bicarbonate	0.951**															
Cl⁻	−0.637**	0.034														
EC	0.884*	0.554	0.068													
F-	−0.346*	−0.190	0.016	−0.169												
Fe	0.739**	0.018	0.215	0.226	−0.035											
NO₃⁻	−0.729	0.343	−0.108	0.215	−0.261	−0.024										
ORP	0.034	0.016	−0.001	0.681**	−0.583	0.081**	0.043									
pH	−0.113	0.092*	−0.176	−0.032	−0.138	−0.105	0.251*	−0.103								
PO₄³⁻	0.043	0.078	−0.02	0.131	0.103	0.036	−0.101	0.058	−0.03							
Salinity	0.020	0.168	0.216*	0.235*	0.773	0.042	0.012	−0.592*	0.004	0.088						
SO₄²⁻	0.886*	−0.089*	−0.03	−0.006	−0.072	−0.114	0.119	0.062	0.323	0.062	−0.014					
TDS	0.224	0.558	0.068	0.986**	−0.168	0.214	0.212*	0.055	−0.01	0.134*	0.238	−0.008				
Temp	0.050	0.239	−0.048	0.180	−0.832	0.033	0.399	0.594	0.235	0.103	−0.663	0.228	0.181			
Total alkalinity	0.651*	1.000**	0.034	0.554*	−0.190**	0.829*	0.343	0.016	0.93*	0.078*	0.168	−0.089	0.558*	0.239		
Total hardness	0.089	0.444	0.197	0.384	−0.140	0.144	0.283	−0.025*	0.206*	−0.005	0.182	0.037	0.39	0.184	0.444	
Water level (ft.)	0.829	−0.392	−0.013	−0.285*	0.066	−0.020	−0.319	0.002	−0.15	−0.073	−0.134	−0.014	−0.288	−0.231	−0.392*	−0.298*

Probability level used: $p < 0.001$**, $p < 0.05$*

As arsenic, *Cl* chloride, *EC* electrical conductivity, *F* fluoride, *Fe* iron, *NO₃⁻* nitrate, *ORP* oxidation reduction potential, *PO₄³⁻* phosphate, *SO₄²⁻* sulphate, *TDS* total dissolved solid

Table 3 Pearson correlation among the various physicochemical parameters of groundwater in post-monsoon season ($n = 174$)

	As (mg/L)	Bicarbonate (mg/L)	Cl⁻ (mg/L)	EC (μS/cm)	F⁻ (mg/L)	Fe (mg/L)	NO₃⁻ (mg/L)	ORP (mV)	pH	PO₄³⁻ (mg/L)	Salinity (ppm)	SO₄²⁻ (mg/L)	TDS (mg/L)	Temp. (°C)	Total alkalinity (mg/L)	Total hardness (mg/L)
Bicarbonate	0.443*															
Cl⁻	−0.855	0.034														
EC	0.822*	0.482*	0.723													
F⁻	−0.221	−0.276	0.255	−0.211												
Fe	0.833**	0.177*	0.215	0.311*	−0.026											
NO₃⁻	−0.821*	0.429	−0.314	0.125	−0.361	−0.011										
ORP	0.029**	0.016*	−0.026	0.068*	−0.512	0.078*	0.043									
pH	−0.211*	0.092	−0.279*	−0.133	−0.223*	−0.107*	0.211	−0.301**								
PO₄³⁻	0.034	0.078	−0.122	0.266	0.112	0.026	−0.101	0.055	−0.031*							
Salinity	0.023	0.168*	0.333	0.112	0.696	0.041	0.013	−0.547	0.006*	0.071						
SO₄²⁻	0.878**	−0.089	−0.125	−0.007	−0.056	−0.124	0.121	0.06	0.347*	0.05	−0.014*					
TDS	0.566**	0.558*	0.336*	0.896*	−0.245	0.199*	0.2	0.050*	−0.022	0.126	0.275	−0.155				
Temp	0.502	0.239	−0.455	0.162	−0.756	0.035	0.412	0.6	0.202	0.114	−0.637	0.103	0.192			
Total alkalinity	0.699*	1.000**	0.221	0.132	−0.132*	0.017	0.332*	0.027*	0.078*	0.082	0.182*	−0.211	0.652*	0.152		
Total hardness	0.755*	0.444	0.236*	0.442*	−0.211*	0.126*	0.212	−0.023	0.211*	−0.007*	0.195	0.772*	0.422*	0.192	0.772*	
Water level (ft.)	0.892	−0.392	−0.513	−0.305	0.0623	−0.018	−0.394	0.001	−0.14	−0.071	−0.122	−0.553	−0.255	−0.242	−0.401	−0.552

Probability level used: $p < 0.001$**, $p < 0.05$*

As arsenic, *Cl* chloride, *EC* electrical conductivity, *F* fluoride, *Fe* iron, *NO₃⁻* nitrate, *ORP* oxidation reduction potential, *PO₄³⁻* phosphate, *SO₄²⁻* sulphate, *TDS* total dissolved solid

Multiple linear regression (MLR) analysis of As

Multiple regression analysis attempts to fit the independent variables for predicting a single dependent variable of groundwater arsenic level and the results are depicted in Eq. (7). From Eq. (7), it has been observed that both iron and manganese showed linear relationship with arsenic level in groundwater (Mogaji et al. 2015). However, the coefficients of both Fe and Mn are not so high ($R^2 < 0.85$). The regression analysis also revealed that the depth and availability of arsenic in groundwater are inversely related ($R^2 = 0.65$).

$$As = 6.28 - 0.772 \times \text{cations} + 0.312 \times \text{anions}$$
$$+ 0.29 \times Fe + 0.33 \times Mn - 0.051 \times \text{water level.} \quad (7)$$

Furthermore, Eq. (7) also indicates the arsenic contamination in groundwater controlled by the availability of cations and anions, derived from the geochemical interaction. Cations appear with negative value, whereas the majority of conversions depict the association of Fe, Mn, and As as anions (Shamsudduha et al. 2015). Conversely, anions show the positive value; hence, MLR analysis revealed that the presence of anions could also imply the arsenic contamination with respect to groundwater depth and aquifer lithology.

Deterministic and probabilistic health risk assessment

The assessment of health risk associated with both consumption and dermal contact of groundwater was represented by IDW interpolating mapping (Elumalai et al. 2017; Yang et al. 2020). The entire health risk due to consumption of groundwater was evaluated with respect to hazard quotient (both ingestion and dermal absorption), average daily dose (ADD), hazard index (HI) and carcinogenic risk (CR). The result revealed that HQ due to ingestion of As-contaminated groundwater ranges from 0.030 to 0.602 with the mean value 0.059 ± 0.057 (SD). Similarly, the HQ due to dermal absorption ranges from 1.305 to 7.025 with the mean value 1.599 ± 0.590 (SD). The ADD, HI and CR also vary from 0.029 to 4.330, 2.290–45.300 and 0.001–0.009 with mean and SD 0.250 ± 0.243, 4.506 ± 4.436 and 0.002 ± 0.0007, respectively (Table 1S). Again, the distribution of hazard quotient with respect to ingestion and dermal absorption is demonstrated in Fig. 6SA and B, respectively. From Fig. 6SA and B, it is clear that the areas of Bhagabangola-1, Beldanga-1, Lalgola and Berhampore are vulnerable with respect to both ingestion and dermal absorption. However, severe HQ was recorded at Farakka, Bhagabangola-2, Bharatpur-2, Beldanga-2 and Murshidabad Jiaganj areas of Murshidabad District (Chowdhury and Paul. 2019; Majumdar 2018). On the other hand, Fig. 7SA also indicates that the ADD is higher in the areas of Farakka, Bhagabangola-2,

Lalgola, Beldanga-2 and Murshidabad Jiaganj, followed by Nawda, Khargram, Sagardighi areas of Murshidabad District. Almost similar outcome was reflected from HI status (Fig. 7SB). Carcinogenic risk is the ultimate outcome for prolonged consumption of such arsenic-contaminated groundwater. In this study, CR was also evaluated and is depicted in Fig. 8SA. Figure 8SA demonstrates that severe carcinogenic risk is most prevalent in the Farakka, Nabagram, Sagardighi, Beldanga-II, Berhampore, Nawda, Khargram and Bharatpur-II areas, followed by Murshidabad Jiaganj, Kandi, and Burwan areas of Murshidabad District. The severity of carcinogenic risk among the inhabitants of the studied areas is possibly due to use of high arsenic-loaded groundwater for drinking, cooking and bathing. Moreover, the groundwater shallow aquifers have shortest thickness of vadose zone where arsenic availability is higher compared to the deep aquifer having larger thickness of vadose zone (Adimalla and Qian 2019; Anim-Gyampo et al. 2019; Hossain and Patra 2020).

The health risk (adult) due to consumption of arsenic-contaminated water was also evaluated trough Monte Carlo simulation modelling which mainly predicts the probability of different outcomes under the availability of various responsible random variables (Table 1S). The beauty of the model is that it explains the impact of risk and uncertainty towards prediction and forecasting of the concerned disease(Li et al.2021). Initially, different health risk indicators such as ADD, HQ and HI were considered as input variables. The model simulation outcomes in the form of deterministic and probabilistic health risk are demonstrated in Table 4. Carcinogenic risk estimation has been considered from the 5th percentile (low risk) and 95th percentile (high risk) based on HI value. At 95% probability, true value lies in the confidence interval (Mondal et al. 2014; USEPA 2012). The higher range of the density function output for carcinogenic risk is being considered as acceptable. Present study results of Monte-Carlo simulation indicates ~ 86.775% probability level of significance, which represents a bit closer to the exceeding threshold values (Fig.8Sb). Moreover, the areas located owing to the exceedance of significant carcinogenic risk are the blocks of Burwan, Nabagram, Sagardighi, Beldanga-II, Kandi, Berhampore, Nawda, Khargram and Bharatpur-II.

Conclusion

The poor quality of arsenic-contaminated groundwater has adverse influence on human health and poses serious threat to the arsenic-prone areas throughout the world. Following the present study, it is observed that all the studied groundwater samples of the Murshidabad District exceeds the WHO's permissible limit of arsenic (0.01 mg/L). The

Table 4 Results of health risk assessment through statistics of the deterministically and probabilistically simulation for groundwater arsenic of average daily dose, hazard quotient, and hazard index through ingestion of groundwater and dermal contact to groundwater

	ADD		HQ		HI
	Ingestion	Dermal	Ingestion	Dermal	
Deterministic approach of risk calculation					
5%	0.131	3.03×10^{-4}	0.339	2.31×10^{-3}	0.468
95%	12.4	0.028	37.7	0.237	37.5
Mean	4.86	0.016	25.6	0.127	22.4
Median	6.16	0.017	27.4	0.132	27.8
SD	3.45	8.85×10^{-3}	24.4	0.073	16.1
Probabilistic simulation of health risk					
5%	0.037	1.15×10^{-4}	0.119	9.33×10^{-4}	0.123
95%	39.5	0.082	111	0.663	1.08×10^{2}
Mean	8.33	0.021	23.1	0.172	25.7
Median	2.42	6.94×10^{-3}	7.53	0.057	6.37
SD	27.8	0.057	67.7	0.463	82.6

analysis of cations and anions revealed alkaline earth metal dominancy is higher than alkali metal. On behalf of aquifer lithology, the observed hydrogeochemical mechanism clearly confines that cation and anion interaction is of the Ca–Mg type, which also support the weathering and dissolution of major rocks from quartzite, hornblende, biotite gneiss and charnockite. According to Gibbs diagram, the predominant ions in groundwater samples fall in the rock–water interaction dominance and evaporation dominance field in the studied area. Moreover, a positive correlation ($p < 0.05$) between arsenic, manganese and iron was recorded. The health risk associated with carcinogenic possibility increases according to arsenic abundances, average daily dose, hazard index, hazard quotient (ingestion and dermal contact of groundwater) and carcinogenic risk. Therefore, on the basis of the quantitative measurement of groundwater physicochemical property, hydrogeochemical interaction, assessing the human health risk followed by USEPA and Monte Carlo simulation method, it may be concluded that the groundwater samples of the studied areas should be checked regularly. The regular monitoring should indicate not only the severity of arsenic manifestation, but also to enumerate the crucial presence of iron and manganese to evaluate the arsenic level in groundwater in Murshidabad District.

Declarations

Conflict of interest All the researchers associated in this research have no conflict of interest to publish this manuscript.

References

Adhikary PP, Dash CJ (2014) Comparison of deterministic and stochastic methods to predict spatial variation of groundwater depth. Appl Water Sci 7(1):339–348. https://doi.org/10.1007/s13201-014-0249-8

Adimalla N, Qian H (2019) Groundwater quality evaluation using water quality index (WQI) for drinking purposes and human health risk (HHR) assessment in an agricultural region of Nanganur, south India. Ecotoxicol Environ Safe 176:153–161. https://doi.org/10.1016/j.ecoenv.2019.03.066

Alam Md, Shaikh WA, Chakraborty S, Avishek K, Bhattacharya T (2016) Groundwater arsenic contamination and potential health risk assessment of gangetic plains of Jharkhand, India. Expos Health 8:125–142. https://doi.org/10.1007/s12403-015-0188-0

Andersen LCD, Bruland KW (1991) Biogeochemistry of arsenic in natural waters: the importance of methylated species. Environ Sci Technol 25(3):420–427

Anim-Gyampo M, Anornub GK, Appiah-Adjeic EK, Agodzod SK (2019) Quality and health risk assessment of shallow groundwater aquifers within the Atankwidi basin of Ghana. Groundw Sustain Dev 9:100217. https://doi.org/10.1016/j.gsd.2019.100217

Anning DW, Paul AP, McKinney TS, Huntington JM, Bexfield LM, Thiros SA (2012) Predicted nitrate and arsenic concentrations in basin-fill aquifers of the southwestern United States: US Geological Survey Scientific Investigations Report 2012–5065, p 78

APHA, AWWA, WEF (2005) Standard methods for examination of the water and wastewater, 21st ed. APHA, Washington, DC (ISBN 0-87553-047-8).

Argos M, Kalra T, Rathouz PJ, Chen Y, Pierce B, Parvez F, Islam T, Ahmed A (2010) Arsenic exposure from drinking water, and all-cause and chronic-disease mortalities in Bangladesh (heals): a prospective cohort study. Lancet 376(9737):252–258. https://doi.org/10.1016/S0140-6736(10)60481-3

Beisner KR, Anning DW, Paul AP, McKinney TS, Huntington JM, Bexfield LM, Thiros SA (2012) Maps of estimated nitrate and arsenic concentrations in basin-fill aquifers of the southwestern United States: US Geological Survey Scientific Investigations Map 3234, pamphlet 8 p., 2 sheets

Bera AK, Rana T, Das S, Bhattacharya D, Bandyopadhyay S, Pan D, De S, Samanta S, Chowdhury AN, Mondal TK, Das SK (2010) Ground water arsenic contamination in West Bengal, India: a risk of sub-clinical toxicity in cattle as evident by correlation between arsenic exposure, excretion and deposition. Toxicol Ind Health 26:709–716. https://doi.org/10.1177/0748233710377775

Bhattacharya P, Ahmed KM, Hasana AM, Alamc M, Bhuyiana M, Khana AA, Sracekd O (2004) Arsenic enrichment in groundwater of the alluvial aquifers in Bangladesh: an overview. Appl Geochem 19:181–200. https://doi.org/10.1016/j.apgeochem.2003.09.006

Bhowmick S, Nath B, Halder D, Biswas A, Majumder S, Mondal P, Chatterjee D (2012) Arsenic mobilization in the aquifers of three

physiographic settings of West Bengal, India: Understanding geogenic and anthropogenic influences. J Hazard Matar 262:915–923. https://doi.org/10.1016/j.jhazmat.2012.07.014

Bhowmick S, Pramanik S, Singh P, Mondal P, Chatterjee D, Nriagu J (2018) Arsenic in groundwater of West Bengal, India: a review of human health risks and assessment of possible intervention options. Sci Total Environ 612:148–169. https://doi.org/10.1016/j.scitotenv.2017.08.216

Bindal S, Singh CK (2019) Predicting groundwater arsenic contamination: regions at risk in highest populated state of India. Water Res 159:65–76. https://doi.org/10.1016/j.watres.2019.04.054

Borah R, Taki K, Gogoi A, Das P, Kumar M (2018) Contemporary distribution and impending mobility of arsenic, copper and zinc in a tropical (Brahmaputra) river bed sediments, Assam, India. Ecotoxicol Environ Safe 161:769–776. https://doi.org/10.1016/j.ecoenv.2018.06.038

Carretero S, Kruse E (2015) Iron and Manganese content in groundwater on the northeastern coast of the Buenos Aires Province, Argentina. Environ Earth Sci 73:1983–1995

Chakraborti D, Das B, Rahman MM, Chowdhury UK, Biswas B, Goswami AB, Nayak B, Pal A, Sengupta MK, Ahamed S, Hossain A, Basu G, Roychowdhury T, Das D (2009) Status of groundwater arsenic contamination in the state of West Bengal, India: a 20-year study report. Mol Nutr Food Res 53:542–551. https://doi.org/10.1002/mnfr.200700517

Chakraborti D, Das B, Rahman MM, Nayak B, Pal A, Sengupta MK, Ahamed S, Hossain MA, Chowdhury UK, Biswas KA, Saha KC, Dutta RN (2017) Arsenic in groundwater of the Kolkata Municipal Corporation (KMC), India: critical review and modes of mitigation. Chemosphere. https://doi.org/10.1016/j.chemosphere.2017.04.051

Chakraborty M, Mukherjee A, Ahmed KM (2015) A review of groundwater arsenic in the Bengal Basin, Bangladesh and India: from source to sink. Curr Pol Rep 1:220–247. https://doi.org/10.1007/s40726-015-0022-0

Chatterjee D, Nath B, Chakraborty S, Majumder S, Biswas A, Bhomick S, Halder D, Mondal D, Kundu A, Saha D, Barman S, Biswas U, Saha I, Das A, Sarkar S, Chatterjee D (2013) Groundwater arsenic in the fluvial Bengal plains: geochemistry and mitigation. Procedia Environ Sci 7:143–146. https://doi.org/10.1016/j.proeps.2013.03.014

Chatterjee R, Samadder S, Mondal D, Adhikari K (2020) Analysis of spatio-temporal trend in groundwater elevation data from arsenic affected alluvial aquifers—case study from Murshidabad district, West Bengal Eastern India. J Earth Syst Sci 129:228. https://doi.org/10.1007/s12040-020-01489-8

Cheng Z, van Geen A, Seddique AA, Ahmed KM (2005) Limited temporal variability of arsenic concentrations in 20 wells monitored for 3 years in Araihazar, Bangladesh. Environ Sci Technol 39:4759–4766. https://doi.org/10.1021/es058017a

Choudhury R, Mahanta C, Verma S, Mukherjee A (2017) Arsenic distribution along different hydrogeomorphic zones in parts of the Brahmaputra River Valley Assam (India). Hydrogeol J 25:1153–1163. https://doi.org/10.1007/s10040-017-1584-2

Chowdhury M, Paul PK (2019) Quantification of groundwater resource of Kandi subdivision of Murshidabad district West Bengal. Environ Dev Sustain. https://doi.org/10.1007/s10668-019-00454-w

Chowdhury UK, Biswas BK, Chowdhury TR, Samanta G, Mandal BK, Basu GC, Chanda CR, Lodh D, Saha KC, Mukherjee SK, Roy S, Kabir S, Quamruzzaman Q, Chakraborty D (2000) Groundwater arsenic contamination in Bangladesh and West Bengal, India. Environ Health Persp 108:393–397. https://doi.org/10.1289/ehp.00108393

Dehnavi AG, Sarikhani R, Nagaraju D (2011) Hydro geochemical and rock water interaction studies in East of Kurdistan, N–W of Iran. Int J Environ Sci Res 1(1):16–22

DeVore CL, Rodriguez-Freire L, Mehdi-Ali A, Ducheneaux C, Artyushkova K, Zhou Z, Latta DE, Lueth VW, Gonzales M, Lewis J, Cerrato JM (2019) Effect of bicarbonate and phosphate on arsenic release from mining-impacted sediments in the Cheyenne River watershed South Dakota USA. Environ Sci Process Impacts. https://doi.org/10.1039/c8em00461g

Dey U, Chatterjee S, Mondal NK (2016) Isolation and characterization of arsenic-resistant bacteria and possible application in bioremediation. Biotechnol Rep 10:1–7. https://doi.org/10.1016/j.btre.2016.02.002

Duggal V, Rani A (2018) Carcinogenic and non-carcinogenic risk assessment of metals in groundwater via ingestion and dermal absorption pathways for children and adults in malwa region of Punjab. J Geol Soc India 92:187–194. https://doi.org/10.1007/s12594-018-0980-0

Ekoa Bessa AZ, Ngueutchoua G, Kwewouo Janpou A et al (2020) Heavy metal contamination and its ecological risks in the beach sediments along the Atlantic Ocean (Limbe coastal fringes Cameroon). Earth Syst Environ. https://doi.org/10.1007/s41748-020-00167-5

Elumalai V, Brindha K, Sithole B, Lakshmanan E (2017) Spatial interpolation methods and geostatistics for mapping groundwater contamination in a coastal area. Environ Sci Pol Res 24:11601–11617. https://doi.org/10.1007/s11356-017-8681-6

Ghosh T, Rolee K (2011) Spatio-temporal pattern of groundwater arsenic concentration in thick unconfined aquifer of Murshidabad District, West Bengal India. Univ J Env Res Technol 1(3):311–319

Ghosh SB, Chakraborty D, Mondal NK (2017) Effect of arsenic and manganese exposure on intellectual function of children in arsenic stress area of Purbasthali, Burdwan West Bengal. Expos Health 9:1. https://doi.org/10.1007/s12403-016-0216-8

Ghosh GC, Khan Md JH, Chakraborty TK, Zaman S, Kabir AHMM, Tanaka H (2020) Human health risk assessment of elevated and variable iron and manganese intake with arsenic safe groundwater in Jashore Bangladesh. Sci Rep 10:5206. https://doi.org/10.1038/s4159s.020-62187-5

Gibbs JR (1970) Mechanisms controlling world water chemistry. Science 80(170):1088–1090

Gogoi A, Tushara Chaminda GG, An AKJ, Snow DD, Li Y, Kumar M (2016) Influence of ligands on metal speciation, transport and toxicity in a tropical river during wet (monsoon) period. Chemosphere 163:322–333. https://doi.org/10.1016/j.chemosphere.2016.07.105

Gotway CA, Feruson RB, Hergert GW, Peterson TA (1996) Comparison of kriging and inverse distance methods for mapping soil parameters. Soil Sci Soc Am J 60:1237–1247

Haldar S (2019) Groundwater arsenic contamination in Murshidabad, West Bengal: current scenario, effects and probable ways of mitigation with special reference to majhyampur water treatment plant, Murshidabad. IOSR J Envron Sci Tox Food Technol 13(6):1–11. https://doi.org/10.9790/2402-1306020111

Herath I, Vithanage M, Bundschuh J, Maity JP, Bhattacharya P (2016) Natural arsenic in global groundwaters: distribution and geochemical triggers for mobilization. Curr Pollut Rep 2:68–89. https://doi.org/10.1007/s40726-016-0028-2

Hossain M, Patra PK (2020) Contamination zoning and health risk assessment of trace elements in groundwater through geostatistical modelling. Ecotoxicol Environ Safe 189:110038. https://doi.org/10.1016/j.ecoenv.2019.110038

Khan SMN, Kumar AR (2013) Geogenic assessment of water quality index for the groundwater in Tiruchengode Taluk, Namakkal district, tamilnadu India. Chem Sci Trans 2(3):1021–1027. https://doi.org/10.7598/cst2013.482

Kim MJ, Nriagu J, Haack S (2002) Arsenic species and chemistry in groundwater of southeast Michigan. Environ Pol 120(2):379–390. https://doi.org/10.1016/s0269-7491(02)00114-8

Kim MJ, Nriagu J, Haack S (2003) Arsenic behavior in newly drilled wells. Chemosphere 52(3):623–633. https://doi.org/10.1016/s0045-6535(03)00244-3

Knierim KJ, Kingsbury JA, Haugh CJ (2021) Machine-learning predictions of redox conditions in groundwater in the Mississippi River Valley alluvial and Claiborne aquifers, south-central United States. US Geological Survey Scientific Investigations Map 3468:16. https://doi.org/10.3133/sim3468.

Kulkarni HV, Mladenov N, Datta S, Chatterjee D (2018) Influence of monsoonal recharge on arsenic and dissolved organic matter in the Holocene and Pleistocene aquifers of the Bengal Basin. Sci Total Environ 637–638:588–599. https://doi.org/10.1016/j.scitotenv.2018.05.009

Kumar M, Kumar P, Ramanathan AL, Bhattacharyay P (2010) Arsenic enrichment in groundwater in the middle Gangetic Plain of Ghazipur District in Uttar Pradesh, India. J Geol Exp 105:83–94. https://doi.org/10.1016/j.gexplo.2010.04.008

Kumar SK, Logeshkumaran A, Magesh NS, Godson PS, Chandrasekar N (2015) Hydrogeochemistry and application of water quality index (WQI for groundwater quality assessment, Anna Nagar, Part of Chennai City, Tamil Nadu India. Appl Water Sci 5:335–343

Kumaresan M, Riyazuddin P (2006) Major ion chemistry of environmental samples around sub-urban of Chennai city. Curr Sci 91(12):1668–1677

Li Y, Ji Li, Mi W, Xie S, Bi Y (2021) Health risks from groundwater arsenic on residents in northern China coal-rich region. Sci Total Environ 773:145003. https://doi.org/10.1016/j.scitotenv.2021.145003

Lim KT, Shukor MY, Wasoh H (2014) Physical, chemical, and biological methods for the removal of arsenic compounds. Biomed Res Int. https://doi.org/10.1155/2014/503784

Liu CN, Wu MZ (2019) Geochemical, mineralogical and statistical characteristics of arsenic in groundwater of the Lanyong Plain Taiwan. J Hydrol 577:123975

Luzati S, Beguraj A, Beguraj GE, Jaujaj O (2016) Iron and manganese in groundwater of Rrogozhina aquifer, Western Albania. J Environ Sci Eng 5:276–285. https://doi.org/10.17265/2162-5263/2016.06.002

Mahato S, Mahato A, Karna PK, Balmiki N (2018) Investigating aquifer contamination and groundwater quality in eastern Terai region of Nepal. BMC Res Notes. https://doi.org/10.1186/s13104-018-3445-z

Majumdar KK (2018) Effect of arsenic safe water on manifestations of arsenicosis. Int J Community Med Public Health 5(10):4573–4577. https://doi.org/10.18203/2394-6040.ijcmph20184012

Majumder S, Datta S, Nath B, Neidhardt H, Sarkar S, Roman-Ross G, Berner Z, Hidalgo M, Chatterjee D, Chatterjee D (2016) Monsoonal influence on variation of hydrochemistry and isotopic signatures: Implications for associated arsenic release in groundwater. J Hydrol 535:407–417. https://doi.org/10.1016/j.jhydrol.2016.01.052

Maliva RG (2019) Anthropogenic aquifer recharge and water quality. Springer Briefs Electr Comput Eng. https://doi.org/10.1007/978-3-030-11084-0_6

Mandal BK, Chowdhury TR, Samanta G, Basu GK, Chowdhury PP, Chanda CR. Lodh D, Karan NK, Dhar RK, Tamili DK, Das D, Saha KC, Chakraborti D (1996) Arsenic in groundwater in seven districts of West Bengal India—the biggest arsenic calamity in the world. Curr Sci 70(11): 976–986. http://www.jstor.com/stable/24111635

Mazumder DG, Dasgupta UB (2011) Chronic arsenic toxicity: studies in West Bengal, India. K J Med Sci 27:360–370

McArthur JM, Ghosal U, Sikdar PK, Ball JD (2016) Arsenic in groundwater: the deep late Pleistocene aquifers of the Western Bengal Basin. Environ Sci Technol 50:3469–3476

Mogaji KA, Lim HS, Abdullah K (2015) Modeling of groundwater recharge using a multiple linear regression (MLR) recharge model developed from geophysical parameters: a case of groundwater resources management. Environ Earth Sci 73:1217–1230. https://doi.org/10.1007/s12665-014-3476-2

Mohammed-Aslam MA, Rizvi SS (2020) Hydrogeochemical characterisation and appraisal of groundwater suitability for domestic and irrigational purposes in a semi-arid region, Karnataka state India. Appl Water Sci 10:237. https://doi.org/10.1007/s13201-020-01320-1

Mondal NK (2020) Prevalence of Arsenic in chicken feed and its contamination pattern in different parts of chicken flesh: a market basket study. Environ Monit Assess 192:590. https://doi.org/10.1007/s10661-020-08558-x

Mondal NK, Chakraborty D, Roy P, Roy TK, Das C, Bhaumik R, Pal KC, Medda S, Datta JK (2014) Correlation between arsenic intoxication and cognitive ability of primary school children of West Bengal. Asia Specif J Trop Dis 4(2):S850. https://doi.org/10.1016/S2222-1808(14)60743-X

Mueller TG, Pierce FJ, Schabenberger O, Warncke DD (2001) Map quality for site-specific fertility management. Soil Sci Soc Am J 65(5):1547–1558

Nakagawa K, Amano H, Persson M, Berndtsson R (2021) Spatiotemporal variation of nitrate concentrations in soil and groundwater of an intensely polluted agricultural area. Sci Rep 11:2598. https://doi.org/10.1038/s41598-021-82188-2

Natasha BI, Shahid M, Niazi NK, Younas F, Naqvi SR, Rinklebe J (2020) Hydrogeochemical and health risk evaluation of arsenic in shallow and deep aquifers along the different floodplains of Punjab Pakistan. J Haz Mat 402:124074. https://doi.org/10.1016/j.jhazmat.2020.124074

National Research Council (US) (1977) Committee on medical and biological effects of environmental pollutants, division of medical sciences and assembly of life sciences. ISBN-10: 0-309-02604-0

Nava-Rivera LE, Betancourt-Martínez ND, Lozoya-Martínez R, Carranza-Rosales P, ElenaGuzmán-Delgado N, Carranza-Torres IE, Delgado-Aguirre H, Zambrano-Ortíz JO, Morán-Martínez J (2021) Transgenerational effects in DNA methylation, genotoxicity and reproductive phenotype by chronic arsenic exposure. Sci Rep 11:8276. https://doi.org/10.1038/s41598-021-87677-y

Neidhardt H, Berner ZA, Freikowski D, Biswas A, Majumder S, Winter J, Norra S (2014) Organic carbon induced mobilization of iron and manganese in a West Bengal aquifer and the muted response of groundwater arsenic concentrations. Chem Geol 367:51–62. https://doi.org/10.1016/j.chemgeo.2013.12.021

Nooria R, Maghrebib M, Mirchic M, Tangd Q, Bhattaraif R, Sadeghg M, Nouryh M, Haghighia AT, Kløvea B, Madanii K (2021) Anthropogenic depletion of Iran's aquifers. PNAS 118(25):e2024221118. https://doi.org/10.1073/pnas.2024221118

O'Day PA, Vlassopoulos D, Root R, Rivera N (2004) The influence of sulfur and iron on dissolved arsenic concentrations in the shallow subsurface under changing redox conditions. PNAS 101(38):13703–13708

Piper AM (1944) A graphic procedure in the geochemical interpretation of water-analyses. Eos Trans Am Geophys Union 25:914–928. https://doi.org/10.1029/TR025i006p00914

Planer-Friedrich HC, Lissner H, Steinborn J, Süß E, Hassan MQ, Zahid A, Alam M, Merkel B (2012) Organic carbon mobilization in a Bangladesh aquifer explained by seasonal monsoon-driven storativity changes. Appl Geochem 27(12):2324–2334

Prathap A, Chakraborty S (2019) Hydro chemical characterization and suitability analysis of groundwater for domestic and irrigation uses in open cast coal mining areas of Charhi and Kuju, Jharkhand India. Groundw Sustain Dev 9:100244. https://doi.org/10.1016/j.gsd.2019.100244

Rahman MM, Sengupta MK, Ahamed S, Lodh D, Das B, Hossain MA, Asad AK (2005) Murshidabad—one of the nine groundwater arsenic-affected districts of West Bengal, India. Part I: magnitude of contamination and population at risk. J Clin Toxicol 43(7):823–834. https://doi.org/10.1080/15563650500357461

Rasool A, Xiao T, Farooqi A, Shafeeque M, Masood S, Ali S, Nasim W (2016) Arsenic and heavy metal contaminations in the tube well water of Punjab, Pakistan and risk assessment: a case study. Ecol Eng 95:90–100. https://doi.org/10.1016/j.ecoleng.2016.06.034

Rowland HAL, Gault AG, Charnock JM, Polya DA (2005) Preservation and XANES determination of the oxidation state of solid-phase arsenic in shallow sedimentary aquifers in Bengal and Cambodia. Mineral Mag 69(05):825–839. https://doi.org/10.1180/0026461056950291

Roy P, Mondal NK, Das B, Das K (2013) Arsenic contamination in groundwater: a statistical modeling. J Urban Environ Eng 7(1):24–29

Roy P, Mondal NK, Das K (2014) Modeling of the adsorptive removal of arsenic: a statistical approach. J Environ Chem Eng 2:585–597

Sahoo HB, Gandre DK, Das PK, Karim MA, Bhuyan GC (2018) Geochemical mapping of heavy metals around Sukinda-Bhuban area in Jajpur and Dhenkanal districts of Odisha India. Environ Earth Sci. https://doi.org/10.1007/s12665-017-7208-2

Samadder SR, Kumar ND, Holden NM (2014) An empirical model to predict arsenic pollution affected life expectancy. Popul Environ 36(2):219–233. https://doi.org/10.1007/s11111-014-0212-5

Selim Reza AHM, Jean JS, Lee MK, Liu CC, Bundschuh J, Yang HJ, Lee YC (2010) Implications of organic matter on arsenic mobilization into groundwater: evidence from northwestern (Chapai-Nawabganj), central (Manikganj) and southeastern (Chandpur) Bangladesh. Water Res 44(19):5556–5574. https://doi.org/10.1016/j.watres.2010.09.004

Shaji E, Santosh M, Sarath KV, Prakash P, Deepchand V, Divya BV (2021) Arsenic contamination of groundwater: a global synopsis with focus on the Indian Peninsula. Geosci Front 12:101079. https://doi.org/10.1016/j.gsf.2020.08.015

Shakoor MB, Bibi I, Niazi NK, Shahid M, Nawaz MF, Farooqi A, Naidu R, Rahman MM, Murtaza G, Luttge A (2018) The evaluation of arsenic contamination potential, speciation and hydrogeochemical behaviour in aquifers of Punjab, Pakistan. Chemosphere 199:737–746. https://doi.org/10.1016/j.chemosphere.2018.02.002

Shamsudduha M, Taylor RG, Chandler RE (2015) A generalized regression model of arsenic variations in the shallow groundwater of Bangladesh. Wat Resour Res 51:685–703. https://doi.org/10.1002/2013WR014572

Shankar S, Shanker U, Shikha (2014) Arsenic contamination of groundwater: a review of sources, prevalence, health risks, and strategies for mitigation. Sci Wor J. https://www.hindawi.com/journals/tswj/2014/304524

Shrivastastava A, Barla A, Yadav H, Bose S (2014) Arsenic contamination in shallow groundwater and agricultural soil of Chakdaha block, West Bengal India. Front Environ Sci 2(50):1–9

Singh AL, Singh VK (2018) Assessment of groundwater quality of Ballia district, Uttar Pradesh, India, with reference to arsenic contamination using multivariate statistical analysis. Appl Water Sci 8:95. https://doi.org/10.1007/s13201-018-0737-3

Singh S, Janardhana RN, Ramakrishna CH (2015) Evaluation of groundwater quality and its suitability for domestic and irrigation use in parts of the Chandauli-Varanasi Region Uttar Pradesh India. J Water Resour Protect. https://doi.org/10.4236/jwarp.2015.77046

Sohrabi N, Kalantari N, Amiri V, Saha N, Berndtsson R, Bhattacharya P, Ahmad A (2020) A probabilistic-deterministic analysis of human health risk related to the exposure to potentially toxic elements in groundwater of Urmia coastal aquifer (NW of Iran) with a special focus on arsenic speciation and temporal variation. Stoch Environ Res Risk Assess. https://doi.org/10.1007/s00477-020-01934-6

USEPA (1989) Risk assessment guidance for superfund volume I: human health evaluation manual (part a) interim final. US Environmental Protection Agency, Office of Emergency and Remedial Response, Washington, DC. USA EPA/540/1-89/002.

USEPA (2004) Risk Assessment Guidance for Superfund, Vol 1, Human Health Evaluation Manual. Part E (Supplemental Guidance for Dermal Risk Assessment). Office of Superfund Remediation and Technology Innovation, Washington, DC. USA EPA/540/R/99/005.

USEPA (2010) US Environmental Protection Agency (EPA) Decontamination research and development conference. US Environmental Protection Agency, Washington, DC. EPA/600/R-11/052, 2011.

USEPA (2012) Drinking Water Standards and Health Advisories. Office of Water. US Environmental Protection Agency, Washington, D.C. USGS, 1993. National Water Summary 190-1991 Stream Water Quality. USGS water supply. 59, 2400

Villalba E, Tanjal C, Borzi G, Páez G, Carol E (2020) Geogenic arsenic contamination of wet-meadows associated with a geothermal system in an arid region and its relevance for drinking water. Sci Total Environ 720:137571. https://doi.org/10.1016/j.scitotenv.2020.137571

Wolf M, Kappler A, Jiang J, Meckenstock RU (2009) Effects of humic substances and quinones at low concentrations on ferrihydrite reduction by geobacter metallireducens. Environ Sci Technol 43(15):5679–5685. https://doi.org/10.1021/es803647r

Wu R, Podgorski J, Berg M, Polya DA (2020) Geostatistical model of the spatial distribution of arsenic in groundwaters in Gujarat State India. Environ Geochem Health. https://doi.org/10.1007/s10653-020-00655-7

Yang W, Zhao Y, Wang D, Wu H, Lin A, He L (2020) Using principal components analysis and IDW interpolation to determine spatial and temporal changes of surface water quality of Xin'anjiang River in Huangshan, China. Int J Environ Res Public Health 17:1–14. https://doi.org/10.3390/ijerph17082942

Zhang Z, Xiao C, Adyeye O, Yang W, Liang X (2020) Source and mobilization mechanism of iron, manganese and arsenic in groundwater of Shuangliao city Northeast China. Water 12:534. https://doi.org/10.3390/w12020534